ELSEVIER

Polymer 42 (2001) 1303–1310

polymer

www.elsevier.nl/locate/polymer

# Synthesis of epoxy–clay nanocomposites: influence of the nature of the clay on structure

X. Kornmann[a], H. Lindberg[b], L.A. Berglund[a,*]

[a]*Division of Polymer Engineering, Luleå University of Technology, S-97187 Luleå, Sweden*
[b]*Division of Wood Material Science, Luleå University of Technology, S-93187 Skellefteå, Sweden*

Received 30 January 2000; received in revised form 25 April 2000; accepted 2 May 2000

**Abstract**

Epoxy–clay nanocomposites were synthesised using two montmorillonite clays (MMT) with different cation-exchange capacities (CEC) (94 and 140 meq/100 g). The purpose was to investigate the influence of the CEC of the clay on the synthesis and structure of epoxy–clay nanocomposites. The dispersion of the 1 nm thick clay layers was investigated by X-ray diffraction (XRD) and transmission electron microscopy (TEM). Although XRD data did not show any apparent order of the clay layers in the nanocomposite, TEM revealed parallel clay layers with interlamellar spacing of 90 Å (MMT of high CEC) and 110 Å (MMT of lower CEC) and the presence of remnant multiplets of non-exfoliated layers. A mechanism responsible for the influence of CEC on nanocomposite interlamellar spacing is discussed. The dispersion of the clay was investigated by SEM and found to be finer in the nanocomposites as compared with in conventional composites although the nanocomposites still have clay aggregates at the microscale rather than a monolithic structure. 

*Keywords*: Nanocomposite; Montmorillonite; Epoxy

## 1. Introduction

Composite materials reinforced on a molecular scale, so-called nanocomposites, are of increasing interest according to an expanding literature. Barrier properties [1,2], fire resistance [3] and increase of mechanical properties [4,5] are a few examples of the advantages provided by this new class of materials. One of the most promising approaches to synthesise these materials consists in dispersing an inorganic clay mineral in an organic polymer on a nanometre scale.

This concept was first introduced by researchers from Toyota [6] who discovered the possibility to build a nanocomposite from polyamide 6 and an organophilic clay. Their new material showed dramatic improvements in mechanical and physical properties. Numerous other researchers later used this concept for nanocomposites based on epoxies [7–9], unsaturated polyester [10], poly($\varepsilon$-caprolactone) [11], poly(ethylene oxide) [12], silicone rubber [13,14], polystyrene [15], polyimide [16], polypropylene [17], poly(ethylene terephthalate) [18], and polyurethane [19]. Those materials were produced either by melt intercalation of thermoplastics or in situ polymerisation. However, full separation of the clay layers in the polymer matrix was only achieved in systems based on polyamide, polyimide and epoxy resins. This is primarily because of fairly high polarity of these prepolymers and curing agents which facilitates diffusion into the organophilic clay galleries. The presence of polar hydroxyl groups in the clay layers impedes non-polar species from fully entering the galleries and exfoliating the clay.

A practical problem in the synthesis of the present class of nanocomposites is to disperse an inorganic clay in an organic medium on a molecular scale. This can be addressed by treating the clay so that it becomes organophilic. Clays such as montmorillonites (MMTs) have a remarkable ability to exchange ions. Their structure consists of two fused silica tetrahedral sheets sandwiching an edge-shared octahedral sheet. Isomorphous substitutions of $Si^{4+}$ for $Al^{3+}$ in the tetrahedral lattice and of $Al^{3+}$ for $Mg^{2+}$ in the octahedral sheet cause an excess of negative charges within the MMT layers. These negative charges are counterbalanced by cations such as $Ca^{2+}$ and $Na^{+}$ situated between the clay layers. An exchange of these cations for alkylammonium ions renders the clay organophilic and lowers the surface energy of the clay layers. It then becomes possible for organic species to diffuse between the layers and eventually

* Corresponding author. Tel.: +46-920-91580; fax: +46-920-91084.
*E-mail address:* lars.berglund@mb.luth.se (L.A. Berglund).

0032-3861/01/$ - see front matter 
PII: S0032-3861(00)00346-3

separate them. The capability of the clay to exchange ions can be quantified by a specific property known as the cation-exchange capacity (CEC). This property is highly dependent on the nature of the isomorphous substitutions in the tetrahedral and octahedral layers and therefore on the nature of the soil where the clay was formed. This explains why montmorillonites from different origins show differences in CEC.

Lan et al. [20] have clarified the mechanism of clay exfoliation in epoxy–clay systems. They argued that the acidity of the alkylammonium ions may catalyse homopolymerisation of the diglycidyl ether of bisphenol A (DGEBA) molecules inside the clay galleries. The CEC of the clay determines the amount of alkylammonium ions present between the clay layers and therefore controls the space available for diffusion of DGEBA molecules during mixing of the organoclay with the epoxy resin. The highest CEC provides the minimum space. In the present study we focus on how the amount of alkylammonium ions intercalated between the clay layers, influences the structure of the resulting nanocomposites. We consider effects of alkylammonium ions on the evolution of the exfoliation process prior to curing (addition of amine). In particular, we compare the effects of two MMTs (with different CEC) on the exfoliation process and the final structure of epoxy-based nanocomposites. The nanostructure is characterised by X-ray diffraction (XRD) and transmission electron microscopy (TEM), whereas the microstructure is observed by scanning electron microscopy (SEM) and compared with the structure of a conventional microcomposite. The microcomposite is based on the same constituents (MMT and epoxy) but since the MMT is untreated, exfoliation of the clay layers does not occur.

## 2. Experimental

### 2.1. Materials

The clays used in this study were a Wyoming type MMT, SWy-2, supplied by the Clay Minerals Depository (University of Missouri) and an industrially purified MMT, CWC, provided by Nanocor Inc. Octadecylamine was provided by Aldrich Chemicals. The epoxy resin was the diglycidyl ether of bisphenol A, EPON 828, provided by Shell Chemicals. It was used in combination with a polyoxyalkylene diamine curing agent, Jeffamine D-230 from Huntsman Corporation.

### 2.2. Purification of the SWy-2 clay

Twenty-five grams of the crude clay were first dispersed into 5 l of 1 N solution of NaCl for 24 h at 70°C to obtain an homoionic clay. It was noted that upon centrifugation of the solution at high speed (3200*g*) an opaque whitish layer accumulates in the bottom of the centrifuge tubes beneath a translucent gel [21]. The analysis of the gel by X-ray revealed that this colloidal suspension contained highly pure MMT whereas the opaque layer contained mainly impurities such as quartz and feldspar. The purity of the gel was further confirmed by chemical analysis using inductively coupled plasma-atomic emission spectroscopy (ICP-AES). The gel was isolated and washed several times with deionised water until no chloride was detected in the centrifugate by one drop of 0.1 N $AgNO_3$ solution. The purified clay was dried at 70°C and stored in a desiccator. The CWC clay was used as received.

### 2.3. Intercalation of the alkylammonium ions

The method was similar to the one used by Usuki et al. [22]. Fifteen grams of the purified SWy-2 clay were dispersed into 1200 ml of distilled water at 80°C. Octadecylammonium chloride $CH_3(CH_2)_{17}NH_3^+ \cdot Cl^-$ was prepared by mixing 5.66 g of octadecylamine $CH_3(CH_2)_{17}NH_2$ with 2.1 ml HCl solution (10 N) in 300 ml distilled water. It was poured in the hot MMT/water solution and stirred vigorously for 1 h at 80°C. A white precipitate formed, was isolated by filtration and washed several times with a hot water/EtOH (50/50) mixture until no chloride was detected in the filtrate by one drop of 0.1 N $AgNO_3$ solution. The octadecylammonium exchanged montmorillonite (C18-SWy-2) was then dried several days at 75°C, ground with a mortar and a pestle, and the $<53\ \mu m$ fraction was collected. The organophilic clay was stored in a dessicator. Long chain alkylammonium ions were chosen because they were shown to favour the formation of exfoliated nanocomposites [23]. A similar procedure was followed to prepare octadecylammonium exchanged CWC (C18-CWC).

### 2.4. Measurements of the cation-exchange capacity

The CEC of both montmorillonites were first measured by determining the amount of alkylammonium salt being retained by the organoclays after careful washing. The dried organophilic clays (C18-SWy-2, C18-CWC) along with a sample of their corresponding untreated clay (SWy-2 and CWC, respectively) were ignited at 1000°C in a furnace. From the differences in the loss on ignition of the sample and blank and the molecular weight of the alkylammonium salt, the milliequivalents (meq) of the organic substance retained by the clays were calculated [24] and those values were taken as their CEC.

Chemical analyses of the two MMTs were also performed by ICP-AES. From these results, the structural formula of each MMT was determined as well as their CEC. The values of the CEC were compared with the previous measurements.

### 2.5. Preparation of epoxy–clay nanocomposites

Prior to curing, the epoxy resin was mixed with the desired amount of organophilic clay at 75°C for several hours. A stoichiometric amount of the curing agent

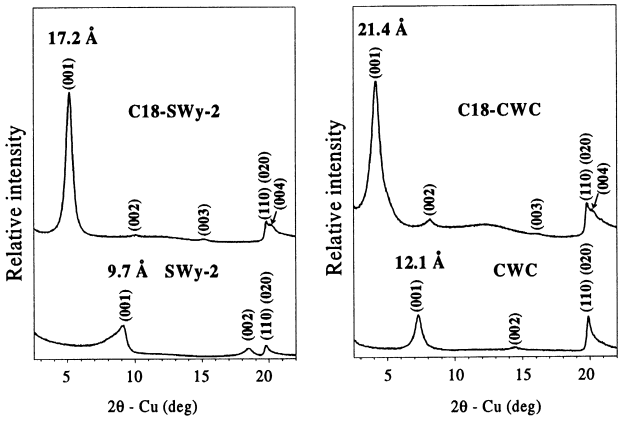


Fig. 1. XRD patterns of the SWy-2 (left) and the CWC (right) clays before (bottom) and after (top) alkylammonium treatment. The spectra are displaced vertically for clarity.

corresponding to 30 wt% of the epoxy resin content was added. The mixture was outgassed in a vacuum oven for a short period of time and poured in a steel mould covered with Mylar A film. All samples were cured for 3 h at 75°C and post-cured 12 h at 110°C. A differential scanning calorimetry analysis of the samples confirmed that they were fully cured.

### *2.6. X-ray diffraction*

Powder XRD analyses were performed using a Siemens D5000 diffractometer with Cu radiation (50 kV, 40 mA). The scanning speed and the step size were 0.08°/min and 0.02°, respectively. The structure of the clay was determined at different stages of the nanocomposite synthesis. The clay powders were mounted on a sample holder with a large cavity and a smooth surface was obtained by pressing the powders with a glass plate. Analyses of the organoclay swollen in the epoxy resin were performed by spreading the mixture on an epoxy disc (50 mm diameter, 2 mm thick) used as sample holder. It was designed so that a maximum surface could be irradiated at low angle, giving an optimum intensity to the XRD signal. The nanocomposite plates produced during the moulding process had a fairly smooth surface. Therefore, disc-shaped specimens (50 mm diameter, 2 mm thick) were cut from these plates and were directly analysed by XRD.

### *2.7. Transmission electron microscopy*

TEM specimens were cut from nanocomposite blocks using an ultramicrotome, LKB 2088 Ultratome V equipped with a diamond knife. Thin specimens, 100–200 nm, were cut from a mesa of about $1 \times 1$ mm$^2$. They were collected in a trough filled with water and placed on 200 mesh copper grids. Transmission electron micrographs were taken with a JEM-2000EX at an acceleration voltage of 200 kV. The image analyses were performed with the software NIH Image 1.61.

### *2.8. Scanning electron microscopy*

The SEM samples were cut from nanocomposite and conventional composite plates and etched for 15 s above a beaker containing hot ethanol. After drying, the samples were coated with a thin layer of carbon and observed in a scanning electron microscope CAMSCAN S4-80DV. The micrographs were obtained using backscattered imaging.

## 3. Results and discussion

### *3.1. Synthesis of the organoclays*

The cation-exchange capacities (CECs) were first measured by determining the amount of alkylammonium salt being retained by the organoclays after careful washing. The CEC for two MMTs, denoted SWy-2 and CWC, were 94 and 140 meq/100 g, respectively. This difference in CEC is probably due to the nature of the isomorphous substitutions present in the tetrahedral and octahedral sheets of the clay [25]. The structural formulae for the two MMTs, derived from their chemical analyses by ICP-AES were $Na_{0.33}K_{0.01}Ca_{0.02}(Mg_{0.26}Fe_{0.23}Al_{1.51})(Al_{0.12}Si_{3.88})O_{10}(OH)_2$ for SWy-2 and $Na_{0.51}K_{0.03}Ca_{0.03}(Mg_{0.36}Fe_{0.14}Al_{1.46})(Al_{0.13}Si_{3.87})O_{10}(OH)_2$ for CWC. The corresponding CEC of SWy-2 and CWC were, respectively, 101 and 159 meq/100 g. The discrepancy between these CECs as compared with the ones obtained by burning the alkylammonium ions may arise from the fact that some interlayer cations in the MMT structure are not exchangeable. These measurements suggest that the CWC clay has a higher layer charge density than the SWy-2. Fig. 1 presents the X-ray diffraction patterns from the SWy-2 and the CWC clays before and after alkylammonium treatment. The interlamellar spacing of the clay, corresponding to the (001) plane peak, increases from 9.7 Å for the purified SWy-2 clay to 17.2 Å for the organophilic clay (C18-SWy-2). This shows that the long chain alkylammonium ions have been intercalated between the layers during the cation-exchange process adopting a lateral bilayer structure [26]. The higher relative intensity of the (001) plane peak is due to a more narrow distribution of the interlamellar spacing when the alkylammonium ions are present. Several basal (00l) reflections can be observed. The peak at high angle ($2\theta = 20°$ $d = 4.5$ Å) remains at a similar position after cation exchange. It corresponds to crystallographic planes of the clay layer, (110) and (020) [27], and its position is independent of the basal spacing. The (001) basal spacing of the CWC clay increases from 12.1 Å for the crude clay to 21.4 Å for the organophilic clay (C18-CWC). According to Weiss [28], the difference in interlamellar spacing between the two organophilic clays (C18-SWy-2 and C18-CWC) arises because the CWC clay has a higher layer charge density than the SWy-2.

Table 1
Basal spacings of the C18-SWy-2 and the C18-CWC organoclays, air dried and swollen in DGEBA at 75°C for different periods of time

| | (001) Basal spacing (Å) | |
|---|---|---|
| | C18-SWy-2 | C18-CWC |
| Air dried | 17.2 | 21.2 |
| Swollen in epoxy at 75°C for | | |
| 5 min | 32.9 | 33.8 |
| 3 h | 33.9 | 34.0 |
| 6 h | 34.7 | 34.0 |
| 12 h | 36.3 | 34.0 |
| 18 h | > 88.0 | 34.0 |
| 24 h | > 88.0 | 34.7 |

### 3.2. Influence of the nature of the clay

The organoclays were swollen in the DGEBA resin for several hours at 75°C. Table 1 presents changes in the (001) basal spacing of the two organophilic clays with swelling duration. After only 5 min of swelling in the epoxy, the interlamellar spacing of both organoclays has increased to a value higher than 30 Å. The hydrophilic nature of the alkylammonium treated clays allows the epoxy molecules to migrate between the layers. The alkylammonium ions have been suggested to reorient from their lateral bilayer structure in the dry state to a perpendicular orientation [20] in order to accommodate the prepolymer. The driving force for this mechanism is controlled by the polarity of the epoxy molecules. The suggested perpendicular orientation is thought to optimise the solvation interactions between the alkyl groups and the DGEBA molecules. As the swelling duration increases up to 24 h, the interlamellar spacing of the C18-CWC clay remains constant (34 Å).

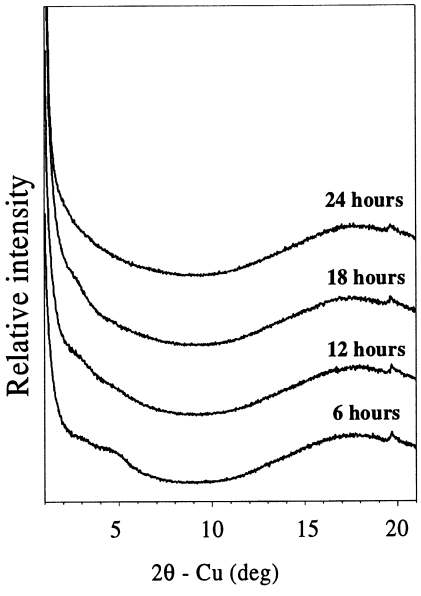


Fig. 2. XRD patterns showing the influence of the swelling duration of the C18-CWC clay in DGEBA at 75°C on the nanocomposite structure. All samples contain 5 wt% of organoclay and were cured 3 h at 75°C and post-cured 12 h at 110°C. The spectra are displaced vertically for clarity.

In contrast, the basal spacing of the C18-SWy-2 clay increases rapidly upon swelling and is not detectable by XRD analysis after 18 h, indicating that the average separation of the layers may be in excess of 88 Å. This could also be because distribution of layer spacings leads to a broad peak which is not clearly visible. Observation of the C18-SWy-2/DGEBA swollen mixture, shows a dramatic increase in viscosity during the mixing. These observations suggest that the C18-SWy-2 clay, but not the C18-CWC clay, initiates a reaction involving the DGEBA molecules, which affects the structure of the clay. A possible mechanism, suggested by Lan et al. [20], is self-polymerisation of the DGEBA resin catalysed by the acidity of alkylammonium ions. The dissociation of the alkylammonium cations, $CH_3(CH_2)_{17}NH_3^+$, in the clay galleries generates protons attacking the epoxide, causing acid catalysed ring opening homopolymerisation. As the polymerisation proceeds further (longer swelling duration), more DGEBA molecules migrate in between the layers. This causes the clay layers to move further apart from each other.

The driving force for the exfoliation process is believed to be the following. The high surface energy of the clay attracts polar species such as DGEBA molecules so that they diffuse in between the layers. If no polymerisation takes place, the system would reach a thermodynamic equilibrium and the layers could not be separated further. As DGEBA molecules react in the proposed homopolymerisation process, they lower their polarity and displace the equilibrium. Then, new polar DGEBA molecules are driven between the layers in order to restore equilibrium. As this mechanism proceeds, the organic molecules driven between the layers exfoliate the clay.

The increase in viscosity during the mixing is then due to the combination of two distinct phenomena: the homopolymerisation of the epoxy as well as the increase in effective clay particle size due to increasing separation of the clay layers. This separation does not occur with the C18-CWC clay. Apparently, the difference in layer charge density between the two MMTs greatly affects the structure of the clay during the swelling phase. This might be explained by the amount of space occupied by the alkylammonium ions in the clay galleries. Indeed, due to its relatively low layer charge density (i.e. low CEC), the C18-SWy-2 clay contains a lower amount of alkylammonium ions. This means that there is more space available for the DGEBA molecules. The self-polymerisation of the DGEBA resin can then occur to a larger extent and causes diffusion of new DGEBA molecules between the clay layers leading to exfoliation of the clay. Furthermore, since a substantial amount of homopolymerisation is apparently taking place in the galleries, the polymer network structure will be inhomogeneous. In particular, we expect excess of amine groups in the network outside the galleries. Homopolymerisation probably also occurs to a limited extent in the galleries of the

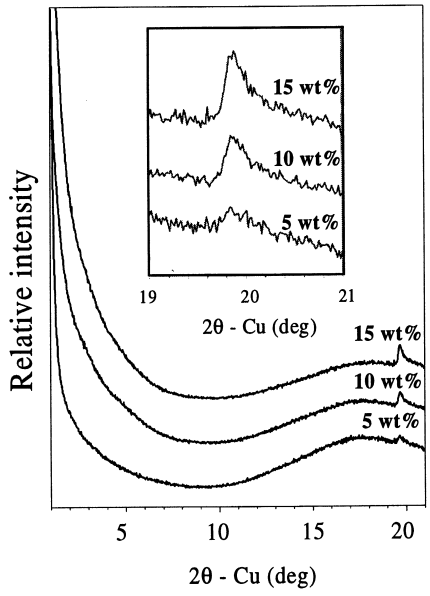


Fig. 3. XRD patterns showing the evolution of the reflection corresponding to the (110) and (020) planes with the organoclay content. The intensity of this peak is proportional to the clay content. The spectra are displaced vertically for clarity.

C18-CWC clay although the limited space restricts the mobility of the DGEBA molecules and prevents a larger spread of the reaction.

### 3.3. Influence of the swelling of the C18-CWC clay in DGEBA resin

The effect of swelling time on clay layer separation in the cured nanocomposite is of interest. In Fig. 2, XRD patterns are presented for Jeffamine D-230 crosslinked epoxy–clay nanocomposites containing 5 wt% of C18-CWC and subjected to different swelling durations prior to curing.

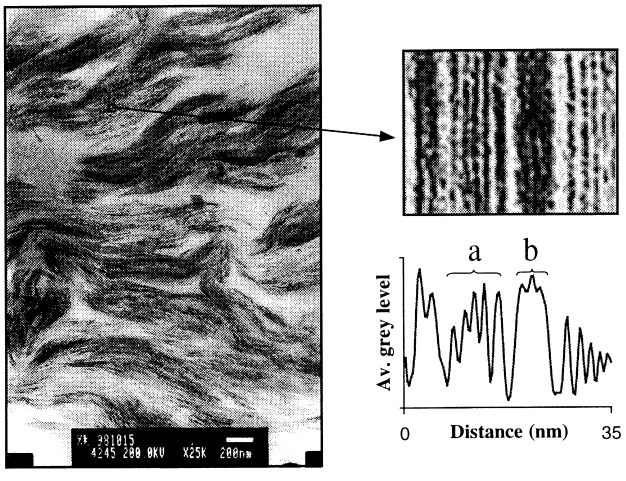


Fig. 4. TEM micrograph of a nanocomposite synthesised with C18-CWC. Image analysis of the enlargement brings to the fore the presence of a stack of (a) intercalated clay and (b) a multiplet of untreated clay (b). The clay content is 5 wt%.

After 6 h of swelling at 75°C and subsequent polymerisation, the XRD pattern shows a large shoulder at low angle. This indicates that a substantial part of the clay is only partially exfoliated. As swelling duration increases, the shoulder progressively disappears and an apparently fully exfoliated structure is obtained after 24 h of swelling and subsequent polymerisation. This last XRD pattern indicates that clay layers are separated by more than 88 Å, the largest basal spacing detectable by XRD. It demonstrates that when the synthesis is carried out with this epoxy system, the organophilic clay needs to be swollen at least 24 h in the DGEBA resin in order to form an apparently fully exfoliated nanocomposite.

Fig. 3 presents the XRD patterns of three nanocomposite samples containing 5, 10 and 15 wt% of organoclay. Even though no (001) basal spacing reflections can be detected at low angle, a peak situated around $2\theta = 20°$ is observed and its intensity increases with the clay content. This peak corresponds to crystallographic planes of the clay layer, (110) and (020). The presence of this peak is important because it demonstrates that the XRD analysis is sufficiently sensitive to detect the presence of the clay in the nanocomposite and to quantify it. This is important in order to allow us to conclude that an exfoliated nanocomposite has been synthesised. Indeed, if the XRD analysis is unable to detect the clay, no (001) peak appears at low angle providing a risk for the misleading conclusion that an exfoliated nanocomposite has been obtained. Detection of the peak corresponding to the (110) and (020) planes prevents this mistake.

### 3.4. Nanocomposite structure

The nanostructure was studied by TEM. Fig. 4 shows the transmission electron micrographs of the nanocomposite synthesised with the C18-CWC clay. The overall picture shows that the clay layers are not occupying the full volume and large regions of pure polymer matrix are visible. At this scale, considerable inhomogeneity is apparent rather than a monolithic structure. A closer observation of the micrograph at high magnification reveals that each dark line often corresponds to several clay layers (3–5). In some cases, this is because the layers are closely stacked together, suggesting the absence of alkylammonium ions in the galleries. In other cases, the layers are intercalated with a *d*-spacing of only around 30 Å (see the enlargement in Fig. 4). The presence of those multiplets was also observed by Akelah et al. in butadieneacrylonitrile/MMT nanocomposites [29]. This interesting detail in the nanostructure demonstrates that the epoxy resin does not diffuse into all the clay galleries during the swelling period. As a consequence, all layers are not separated individually upon polymerisation. The average distance between the stacks of layers evaluated from the overall picture is around 90 Å. This is in good agreement with XRD results where no basal (00l) reflection is observed. XRD is unable to detect regular stacking exceeding 88 Å. One may note that the

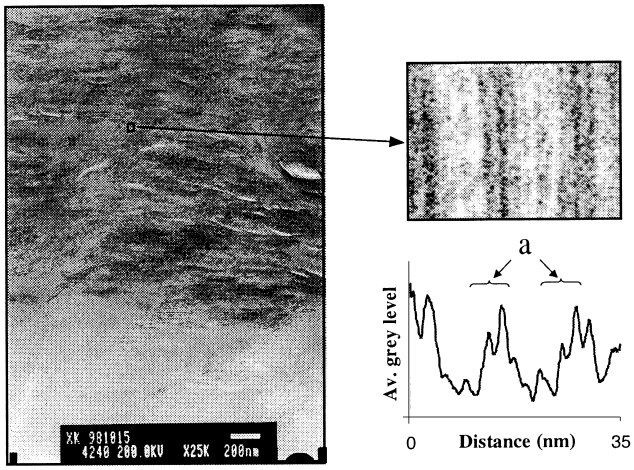


Fig. 5. TEM micrograph of a nanocomposite synthesised with C18-SWy-2. Image analysis of the enlargement reveals the presence of stacks of intercalated clay (a) at about 11 nm distance from each other. The clay content is 5 wt%.

commonly used definition of an exfoliated nanocomposite is based on a layer spacing larger than this value. In reality, TEM micrographs tell us, also a nanocomposite with a layer spacing larger than this value shows regular spacing and is of very similar structural nature as an intercalated composite.

Fig. 5 presents a TEM micrograph of a nanocomposite synthesised with C18-SWy-2 clay. A similar arrangement of the layers as in Fig. 4 is observed with the presence of multiplets (see enlargement in Fig. 5). The average distance between the stacks of layers is about 110 Å. The difference in morphology of the two clays in their nanocomposites is apparently due to self-polymerisation of the DGEBA resin induced by the C18-SWy-2 clay during the swelling phase.

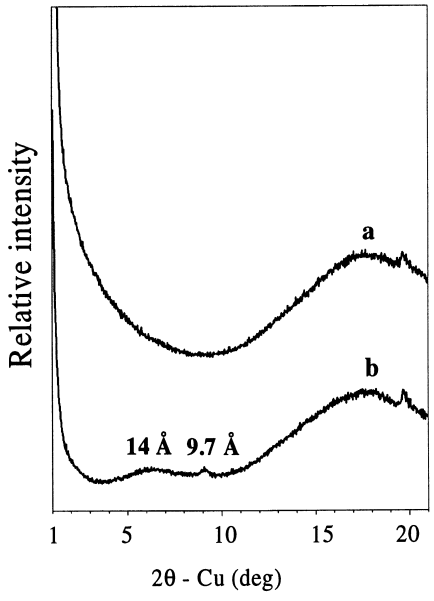


Fig. 6. XRD patterns of (a) an exfoliated nanocomposite and (b) a conventional composite where the clay (CWC) is added as a conventional filler. The clay content is 5 wt%. The spectra are displaced vertically for clarity.

Indeed, when the polymerisation is initiated by addition of the curing agent, self-polymerisation of the resin has already separated the layers significantly (>88 Å). Addition of the curing agent and the associated polymerisation may separate the layers further apart as compared with the C18-CWC clay.

The distribution in layer spacing is also apparent from the TEM micrographs. This is important to keep in mind as XRD data are interpreted and has perhaps not been fully appreciated in the past. Our previous interpretation of XRD data therefore needs some clarification. Although it is common practice to classify a nanocomposite as fully exfoliated from the absence of (00l) reflections, TEM micrographs reveal a more complex situation. The average layer spacing may even be smaller than 88 Å, where the absence of (00l) reflections is primary caused by a wide distribution in layer spacings. Indeed, a very wide distribution in layer spacing would result in smooth shoulders rather than distinct peaks in the XRD spectrum.

### *3.5. Comparison between a nanocomposite and a conventional composite structure*

Fig. 6 presents the XRD pattern of an exfoliated nanocomposite using C18-CWC compared with the one obtained with a composite where the crude clay (CWC) has been added as a normal filler. The comparison of the peak situated at $2\theta = 20°$ suggests that a similar amount of clay is embedded in the epoxy resin. The difference between the two structures is observable in the diffraction patterns obtained at lower angle. Indeed, whereas the nanocomposite shows no basal reflection, the conventional composite shows two peaks: a broad peak corresponding to a *d*-spacing of 14 Å and a sharp one corresponding to a *d*-spacing of 9.7 Å. The sharp peak corresponds to the interlamellar spacing of the dry clay. The broad peak is related to the presence of clay in the hydrated state. Hydration of the

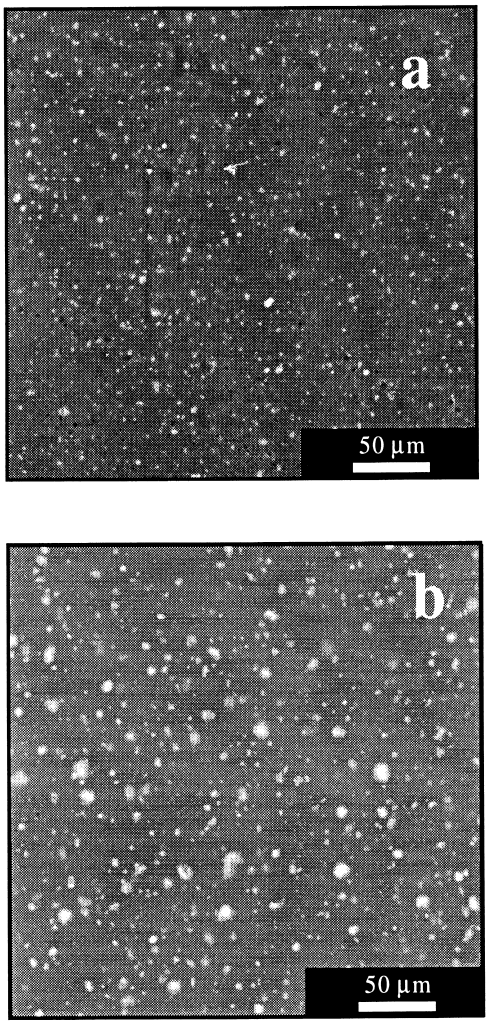


Fig. 7. SEM micrographs of (a) an exfoliated nanocomposite and (b) a conventional composite where the clay (CWC) is added as a normal filler. The clay content is 5 wt%.

crude clay occurs during the swelling phase and may be due to the presence of water molecules in the epoxy resin.

Fig. 7 presents the microstructures of these two materials observed by SEM. The bright spots on the backscattered images correspond to clay aggregates. Fig. 7a presents the microstructure of a nanocomposite with 5 wt% of organoclay. The clay particles are finely dispersed in the material. Moreover, the finest dispersion can probably not be detected by SEM. In the conventional composite (Fig. 7b), large aggregates around 10 μm in diameter are observed. Apparently, the clay particles are more finely dispersed in the nanocomposite as compared with in the conventional composite. This difference must be due to the treatment of the clay. The alkylammonium ions render the clay organophilic and allow a better dispersion of the clay in an organic medium. However, it is interesting to note that the nanocomposite does not show a monolithic structure as defined by Lan et al. [23]. Small particle aggregates are observable at relatively low magnification. This is very important in the context of mechanical properties where the microstructure rather than the nanostructure may control several phenomena.

## 4. Conclusions

The cation-exchange capacity of the clays is of importance in the synthesis of epoxy–clay nanocomposites because it determines the amount of alkylammonium ions, which can be intercalated between the layers. In this context, the swelling phase is of critical importance to the final nanocomposite structure. An MMT with a low CEC (94 meq/100 g) is exfoliated already during swelling in the epoxy resin prior to curing. A possible mechanism explaining this phenomenon is homopolymerisation of the epoxy resin during the swelling phase, causing diffusion of new epoxy molecules into the clay galleries. The large amount of space available between the layers favours the diffusion. The swelling duration of the clay with high CEC (140 meq/100 g) is shown to be critical for the synthesis of an exfoliated nanocomposite.

Regarding the structure, TEM micrographs reveal interlamellar spacing of 90 Å (low CEC) and 110 Å (high CEC). However, multiplets of non-exfoliated layers were also observed. Although it is common practice to classify a nanocomposite as fully exfoliated from the absence of (00l) reflections, these micrographs reveal a more complex situation. The large distribution of basal spacings may, in fact, cause the absence of (00l) reflections. In summary, these nanocomposites contain clay-polymer composite particles consisting of inhomogeneously distributed silicate layer aggregates with polymer between these layers.

On the microscale, the nanocomposites do not present a monolithic structure either, although the SEM micrographs demonstrate a finer dispersion of the clay particles in the nanocomposite as compared with the conventional composite based on the same constituents. Since fracture properties may be controlled by microscale phenomena, this emphasises the need to also optimise the structure on the microscale as new nanocomposite materials are developed.

## Acknowledgements

This work was financially supported by the Swedish Research Council for Engineering Sciences (TFR). The staff of the Division of Chemical Technology at Luleå University of Technology is gratefully acknowledged.

## References

[1] Kojima Y, Usuki A, Kawasumi M, Okada A, Kurauchi T, Kamigaito O. J Appl Polym Sci 1993;49:1259.
[2] Yano K, Usuki A, Okada A. J Polym Sci: Polym Chem 1997;35:2289.
[3] Gilman JW, Kashiwagi T, Brown JET, Lomakin S, Giannelis EP,

Manias E. Proceedings of the 43rd International SAMPE Symposium Part I, vol. 43, 1998. p. 1053.
[4] Okada O, Usuki A. Mater Sci Engng C 1995;3:109.
[5] Wang Z, Pinnavaia TJ. Chem Mater 1998;10:1820.
[6] Okada O, Kawasumi M, Usuki A, Kojima Y, Kurauchi T, Kamigaito O. Mater Res Soc Symp Proc 1990;171:45.
[7] Pinnavaia TJ, Lan T, Wang Z, Shi H, Kaviratna PD. ACS Symp Ser 1996;622:250.
[8] Messersmith PB, Giannelis EP. Chem Mater 1994;6:1719.
[9] Kelly P, Akelah A, Qutubuddin S, Moet A. J Mater Sci 1994;29(9):2274.
[10] Kornmann X, Berglund LA, Sterte J, Giannelis EP. Polym Engng Sci 1998;38:1351.
[11] Messersmith PB, Giannelis EP. Chem Mater 1993;5:1064.
[12] Messersmith PB, Giannelis EP. J Polym Sci: Polym Chem 1995;33:1047.
[13] Burnside S, Giannelis EP. Chem Mater 1995;7:1597.
[14] Wang S, Long C, Wang X, Li Q, Qi Z. J Appl Polym Sci 1998;69:1557.
[15] Vaia RA, Ishii H, Giannelis EP. Chem Mater 1993;5:1694.
[16] Yano K, Usuki A, Okada A, Kurauchi T, Kamigaito O. J Polym Sci: Polym Chem 1993;31:2493.
[17] Hasegawa N, Kawasumi M, Kato M, Usuki A, Okada A. J Appl Polym Sci 1997;63:137.
[18] Ke Y, Long C, Qi Z. J Appl Polym Sci 1997;1:1139.
[19] Wang Z, Pinnavaia TJ. Chem Mater 1998;10:3769.
[20] Lan T, Kaviratna PD, Pinnavaia TJ. J Phys Chem Solids 1996;57:1005.
[21] Barshad I. Soil Sci 1969;107:337.
[22] Kawasumi M, Hasegawa N, Kato M, Usuki A, Okada A. Macromolecules 1997;30:6333.
[23] Lan T, Kaviratna PD, Pinnavaia TJ. Chem Mater 1995;7:2144.
[24] McAtee JL. Am Mineral 1959;44:1230.
[25] Grim RE. In: Press F, editor. Clay mineralogy, 2nd ed.. New York: McGraw-Hill, 1968. p. 194.
[26] Lagaly G. Solid State Ionics 1986;22:43.
[27] Earley JW, Osthaus BB, Milne IH. Am Mineral 1953;38:707.
[28] Weiss A. Angew Chem Int Ed Engl 1963;2:134.
[29] Akelah A, Salahuddin N, Hiltner A, Baer E, Moet A. Nanostruc Mater 1994;4:965.